# Role of *X* valley on the dynamics of electron transport through a GaAs/AlAs double-barrier structure

H. V. A. Galeti,[1] H. B. de Carvalho,[2,*] M. J. S. P. Brasil,[2] Y. Galvão Gobato,[1] V. Lopez-Richard,[1] G. E. Marques,[1] M. Henini,[3] and G. Hill[4]

[1]*Departamento de Física, Universidade Federal de São Carlos, 13565-905, São Paulo, Brazil*
[2]*Instituto de Física "Gleb Wataghin," Universidade Estadual de Campinas-UNICAMP, 13083-970, Campinas, São Paulo, Brazil*
[3]*School of Physics and Astronomy, University of Nottingham, NG7 2RD, United Kingdom*
[4]*EPSRC National Centre for III-V Technologies, University of Sheffield, S1 3JD, United Kingdom*

(Received 21 May 2008; published 8 October 2008)

The transport of electrons through a GaAs/AlAs double-barrier structure with *p*-type doped contacts was investigated using time-resolved photoluminescence spectroscopy. Under illumination, the current-voltage characteristics of the device present two additional features attributed, respectively, to resonant Γ-Γ and Γ-*X* electron tunneling. Optical measurements for biases where these two alternative transport mechanisms have competitive probabilities revealed an unusual carrier dynamics. The quantum well emission is strongly delayed and we observe a remarkable nonlinear effect where the emission intensity decreases at the arrival of a laser pulse. We propose a simple model that adequately describes our results where we assume that the indirect-transition rate depends on the density of electrons accumulated along the structure.

DOI: 10.1103/PhysRevB.78.165309 PACS number(s): 73.40.Gk, 78.47.Cd, 78.67.De, 78.55.Cr

Resonant tunneling diodes (RTDs) have attracted a large interest for various decades due to their potential to investigate basic physics phenomena and for applications in optoelectronic devices.[1] Recently, the interest in those structures has gained a new impulse as it has been proposed to use RTD structures for developing spin filter devices.[2–7] Particularly, several earlier studies have been performed in GaAs/AlAs resonant tunneling diodes.[1] AlAs is an indirect-gap material with the minima of conduction band at *X* points of Brillouin zone, whereas in GaAs the minimum is at Γ point. Therefore, the energy profile of the *X* minimum in the conduction band along the GaAs/AlAs structure forms a quantum well (QW) for electrons in the AlAs layers. It was shown experimentally that resonant tunneling through *X*-valley levels results in additional peaks in the current-voltage characteristic curves.[8–11]

In addition to transport measurements, optical recombination is a useful tool to study fundamental points related to the resonant tunneling of carriers and the charge buildup in RTDs.[12] Furthermore, time-resolved photoluminescence (PL) can also be applied to investigate the tunneling of carriers through double-barriers structures.[13–17] For instance, the tunneling character of the transport of carriers through RTD structures has been confirmed by time-resolved PL measurements where it was observed that tunneling rates increase for narrower barriers and higher applied biases while they are mainly independent of the temperature.[13–15] Measured PL decay times in RTD structures were typically of the order of 50–500 ps, even though anomalous slow transients have been observed for AlAs/GaAs double-barrier structures,[16,17] which was ascribed to the trapping of photocreated carriers in the triangular potential wells adjacent to the barriers followed by nonresonant tunneling to the QW.

In this work we study the dynamics of minority electrons photocreated in a *p*-*i*-*p* AlAs/GaAs RTD structure using time-resolved PL. Evidences of Γ-Γ and Γ-*X* tunneling of photogenerated electrons through the structure were obtained on the $I(V)$ characteristics curve. The QW emission also presents two bands, which we associated, respectively, to direct Γ-Γ and indirect *X*-Γ transitions. For bias voltages close to the feature associated to Γ-*X* electron tunneling, the lower energy band becomes strong and the transients show an unusual behavior. At those voltages, the QW response becomes slower than the laser repetition. Therefore, the PL intensity is still significant when the next laser pulse hits the sample. Immediately after a laser pulse the QW emission intensity does not present, however, an abrupt increase as expected due to the additional number of photocreated carriers. Instead, it abruptly decreases followed by a long rise time. We analyze our results considering the role of the Γ-*X* transfer in the tunneling of electrons through the AlAs barriers.

The sample was grown by molecular-beam epitaxy and consists of a 4.2 nm GaAs QW surrounded by two AlAs tunnel barriers with distinct thicknesses (4.5 and 5.7 nm) and by two identical GaAs spacer layers (5.1 nm).[18] The above structure is surrounded by a set of *p*-GaAs contact layers with increasing doping on each side. The total thickness of the topping GaAs layer over the AlAs barrier is 800 nm. Circular mesas of 400 $\mu$m diameter with AuGe annular top contacts were processed to allow optical measurements under applied bias. Time-resolved PL measurements were performed at 2 K using a 67 MHz ps Ti: Sapphire laser tuned at 1.55 eV and a streak camera.

A schematic band diagram of the sample is presented in Fig. 1 under bias (positive in our convention). We present the profiles of the conduction-band minima at both the Γ and *X* points of the Brillouin zone. For electrons in the Γ band, the AlAs layers act as barriers and the thin GaAs layer as a QW; while in the *X* profile, the AlAs layers act as QWs and the GaAs layers as barriers. Electron transport along the structure can thus arise by either tunneling through the Γ AlAs barrier or by intervalley tunneling via the *X* AlAs confined states. Intervalley transport has been previously investigated and demonstrated in AlAs/GaAs structures.[8–11]

Figure 2 shows the $I(V)$ characteristics when our structure is in the dark and illuminated by the pulsed laser. The two peaks observed under dark conditions are attributed to reso-

 ©2008 The American Physical Society

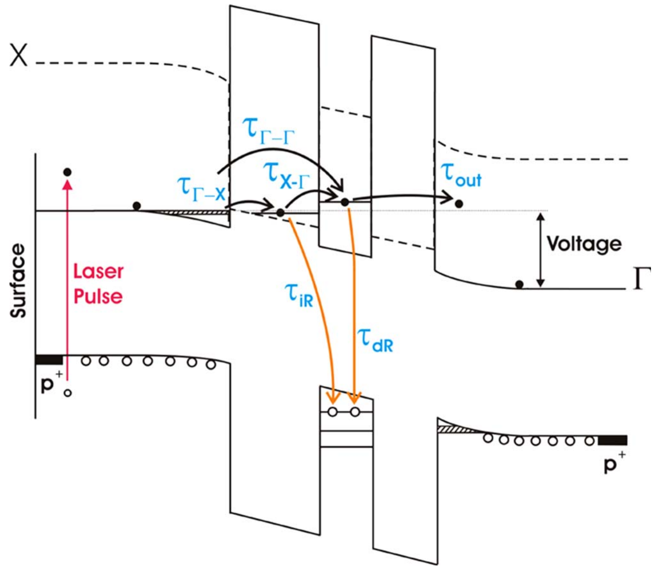


FIG. 1. (Color online) Schematic band diagram of our structure under positive bias showing the profiles of the conduction-band minima at the Γ and $X$ points of the Brillouin zone.

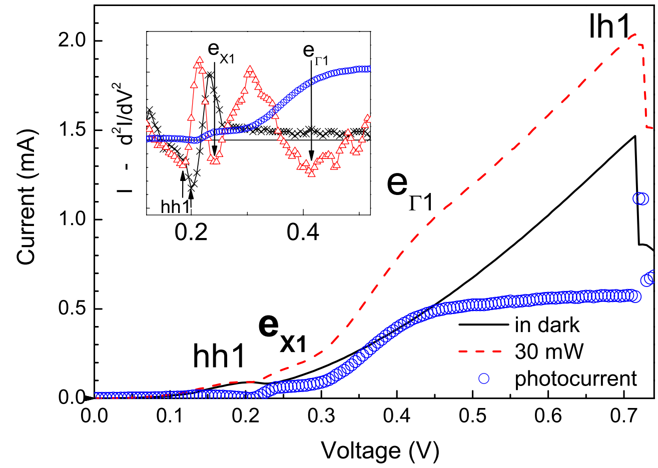


FIG. 2. (Color online) $I(V)$ curve in the dark (continuous line) and under 30 mW laser illumination (dashed line), and the photocurrent (open circles) obtained by subtracting the current with and without laser excitation. The inset presents the photocurrent data for a selected voltage range and the second derivative of the $I(V)$ curves in the dark (crosses) and under illumination (triangles).

nant tunneling through the hh1 and lh1 QW hole subbands.[18] Under light excitation, we observe the development of two additional features at ~0.24 V and ~0.42 V that are more clearly observed in the photocurrent curve obtained by subtracting the current with and without laser excitation also shown in Fig. 2. In order to convert those voltages on energy, we considered a linear dependence between applied bias and energy, which was obtained using the experimental hole-resonances bias voltages and the calculated hole-energy levels. This is a rather simple model that does not consider the charge buildup in the RTD structure. However, it is only used to obtain a rough estimative of the energy of the level related to the $IV$ feature in order to compare it with the PL results. We thus estimate an energy separation between the two levels associated to the photocreated features of ~22 meV, which is much smaller than the expected energy separation between the first and second GaAs QW electron levels. We attribute the peak at ~0.42 V to the resonant tunneling of photogenerated electrons through the fundamental QW state ($e_{\Gamma 1}$) and the ~0.24 V feature to the transfer of electrons via the lowest energy state confined at the AlAs $X$ well ($e_{X1}$).

Under positive bias, electrons created by the laser pulse are injected through the barriers and may recombine with majority holes at the $p$-contact layers and also with holes accumulated at the GaAs QW. The time-resolved PL emission thus reflects the dynamics of the photocreated minority electrons through our structure. We point out two main recombination transitions involving holes confined at the GaAs QW (see Fig. 1): a direct transition with electrons confined at the Γ GaAs QW and an indirect one both in real space and momentum involving electrons localized at the $X$ AlAs layer. We remark that even if the oscillator strength of the direct recombination should be significantly larger than that of the indirect recombination, the intensity of those recombination channels may become comparable depending on the tunneling conditions and the resulting density occupation of the electronic states related to those transitions. Other recombination transitions involving, for instance, electrons, at the second $X$ AlAs layer and holes at the Γ GaAs accumulation layer are also possible, but we did not observe any PL emission that might be associated to those transitions.

Figure 3 summarizes the results of time-resolved PL measurements. The first column shows streak camera images from the QW emission for various distinct bias voltages. The horizontal and vertical axes of the images correspond, respectively, to emission wavelength and time. The PL intensity is represented by a color scale. The total time window is 20 ns, which includes two laser-pulses view as dark lines in the image due to a software procedure adopted to subtract the residual scattered laser pulse. The second column presents PL spectra obtained from each image by integrating the emission intensity for certain constant time intervals. Some spectra clearly comprise two emission bands separated by ~5 meV, which we attribute to the direct Γ-Γ ($E_d$) and indirect $X$-Γ ($E_i$) QW transitions, based on the following discussion. The apparent discrepancy between the energy separation of fundamental $X$ and Γ confined levels estimated by the $I(V)$ characteristics (22 meV) and that obtained from the PL results (5 meV) can be attributed to the fact that the PL emission corresponds to the recombination of an electron-hole pair while the tunneling process only involves electron energy levels. Moreover, the binding energy between an indirect AlAs-GaAs electron-hole pair should be negligible as compared to the binding energy of the direct exciton formed at the thin GaAs QW, which should be of the order of the energy difference between the two energy values mentioned above. We also remark that the lower energy band shows a small blue shift (~1 meV) for increasing times. The shift is probably related to the variation of the density of photogenerated electrons with time, which by its turn changes the energy of the PL emission due to the variation of the electric field along the structure, and to other possible density-dependent effects such as band-gap renormalization and for-

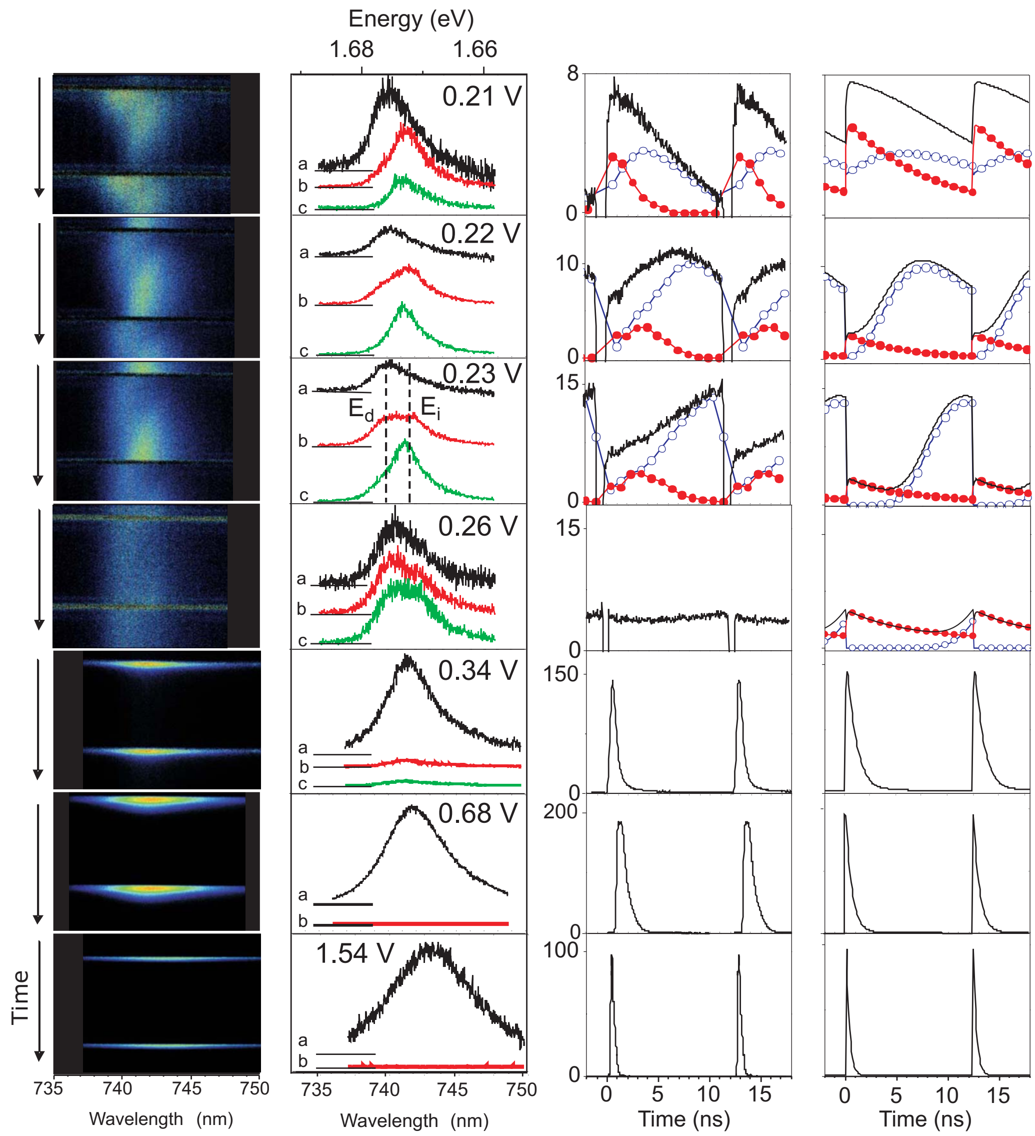


FIG. 3. (Color online) First column: streak camera images from the QW emission for various distinct bias voltages. The horizontal and vertical axes of the images correspond, respectively, to emission wavelength and time. The time window of each image is 20 ns. PL intensity is represented by a gray (color) scale normalized for each image. Second column: time integrated PL spectra for various distinct 2 ns time windows: (a) 0–2 ns, (b) 4–6 ns, (c) 8–10 ns. The spectra were vertically shifted by adding constants that correspond to the short lines at the left side of the figure. Third column: The continuous line is the PL transient obtained by integrating the PL signal for the whole wavelength interval. The open/solid circles transients correspond to the integrated intensity of the lower energy-indirect $X$-$\Gamma(E_i)$ /higher energy-direct $\Gamma$-$\Gamma(E_d)$ QW emission bands obtained by fitting the PL spectra corresponding to 1 ns time windows with two Gaussian bands. Fourth column: simulations obtained by solving the proposed system of rate equations with the set of parameters presented in Table I. The symbols follow the same notation as used for the third column.

mation of excitonic complexes. The discerning of those effects requires a quantitative analysis of this rather complex problem, which is still under progress.

The third column presents PL intensity transients obtained by integrating the PL emission for the whole wavelength interval. For those bias voltages where the two emission bands can be resolved, we also present the intensities for each band obtained by fitting the PL spectra for various time intervals with two Gaussian bands. For voltages up to ~0.30 V, the PL transients present rather unusual characteristics that will be discussed in details along this work. For biases larger than 0.30 V, the QW emission is mainly due to a single band, and the transients present a more conventional behavior. For voltages up to ~0.70 V, the dominant decay time is of the order of 500 ps and the PL intensity increases with biases indicating an increasing number of carriers tunneling into the QW. For higher voltages, the decay time decreases up to ~150 ps and the PL intensity decreases eventhough the current continues to increase, which is consistent with an increasing efficiency for carriers tunneling out of the QW.

We now analyze the carrier dynamics for low voltages where the PL spectra are clearly composed of two emission bands. The low-energy band shows a maximum at ~0.23 V around the same voltage of the $I(V)$ feature attributed to the $\Gamma$-$X$ tunneling of electrons, which corroborates its assignment to the indirect recombination of electrons confined at the AlAs layer ($X$ point) and holes confined at the GaAs layer ($\Gamma$ point). The rising of this emission band is anomalous, slow, and, contrary to the predictable behavior, it becomes increasingly slower as the bias approaches the value at which the emission intensity reaches its maximum. For voltages around 0.23 V, the rising time becomes longer than the laser repetition period, and the PL transient shows a remarkable effect. The low-energy emission band shows a non-null intensity at the end of a time window but its intensity abruptly decreases when the next laser pulse arrives. This nonlinear effect goes against the expected increase in intensity due to additional carriers generated by a light pulse.

PL transients from RTD structures are usually described using a simple model, which considers that the carriers are instantaneously created at the accumulation layer by the laser pulse. The photocreated carriers can thus tunnel into the QW with a probability $\tau_{t1}^{-1}$ and subsequently recombine with a probability $\tau_r^{-1}$ or tunnel out of the QW through the second barrier with a probability $\tau_{t2}^{-1}$.[13,14] The resulting rate equations give a solution of the form for the PL transients,[14]

$$I(t) = I_o[\exp(-t/\tau_{t1}) - \exp(-t/\tau_{\text{eff}})]/(\tau_{t1} - \tau_{te}), \quad (1)$$

where $1/\tau_{\text{eff}}=1/\tau_{t2}+1/\tau_r$. The exponential function with the shortest (longest) time constant represents the rise (decay) of the PL intensity. We remark that if just one of the time constants involved in Eq. (1) is small, it would result in a short rising-time transient.

In principle, even in the presence of two parallel transport mechanisms, this model could still be applied to each of them separately as long as the processes are independent. However, in order to obtain such slow transients observed at low voltages, it would require unusually long-time constants for all the processes involved at those voltages. This was assumed in previous works where the long-time constants were attributed to nonresonant tunneling processes.[16,17] However, in order to describe our results, we would have to consider time constant values that become larger as we approach the resonant voltage attributed to the $\Gamma$-$X$ transfer, which is physically unreasonable and would not result in the photocurrent peak at $\sim$0.23 V. Finally, the model above cannot explain the observed abrupt decreasing of PL intensity generated by a laser pulse.

We thus consider a more detailed model, which takes into account two coupled recombination channels giving rise to the following rate equations for the density of electrons at the accumulation layer ($n_a$), at the $X$ confined state, at the AlAs layer ($n_X$), and at the $\Gamma$ GaAs QW ($n_\Gamma$):

$$\frac{dn_a}{dt} = -\frac{n_a}{\tau_{\Gamma\text{-}X}} - \frac{n_a}{\tau_{\Gamma\text{-}\Gamma}}, \quad (2)$$

$$\frac{dn_X}{dt} = \frac{n_a}{\tau_{\Gamma\text{-}X}} - \frac{n_X}{\tau_{X\text{-}\Gamma}} - \frac{n_X}{\tau_{iR}}, \quad (3)$$

$$\frac{dn_\Gamma}{dt} = \frac{n_a}{\tau_{\Gamma\text{-}\Gamma}} + \frac{n_X}{\tau_{X\text{-}\Gamma}} - \frac{n_\Gamma}{\tau_{dR}} - \frac{n_\Gamma}{\tau_{\text{out}}}, \quad (4)$$

where $1/\tau_{\Gamma\text{-}X}$ is the transfer rate of electrons from the $\Gamma$ GaAs accumulation layer to the $X$ AlAs layer; $1/\tau_{\Gamma\text{-}\Gamma}$ is the probability of tunneling from the $\Gamma$ GaAs accumulation layer to the $\Gamma$ GaAs QW; $1/\tau_{\text{out}}$ is the probability of tunneling out of the $\Gamma$ GaAs QW; $1/\tau_{X\text{-}\Gamma}$ is the transfer rate from the $X$ AlAs layer to the $\Gamma$ GaAs quantum well; $1/\tau_{iR}$ is the indirect $X$-$\Gamma$ radiative recombination rate; and $1/\tau_{dR}$ is the direct $\Gamma$-$\Gamma$ radiative recombination rate. Furthermore, we propose that the radiative recombination rate of the spatially and momentum-indirect $X$-$\Gamma$ recombination between electrons confined at the AlAs $X$ band and holes confined at the $\Gamma$ GaAs QW depends on the concentration of carriers at the accumulation layer given by

$$\tau_{iR} = \tau_{iRo}(1 + e^{(n_a - n_a^*)/\Delta n_a}), \quad (5)$$

where $n_a^*$ represents a critical density behind, which the probability of the indirect recombination abruptly decreases, and $\Delta n_a$ determines the abruptness of this effect. This assumption is essential to generate the observed nonlinear effect and it can be justified considering that the presence of a large density of electrons should affect the electric field, the alignment of the confined levels of our structure, and the critical bounding between an electron-hole pair at different spaces and with different momentum. The resulting system of differential equations can be solved numerically. The large number of parameters of this model makes it useless for a strict fitting procedure, but we can test if it reproduces the experimental results with an appropriate set of parameters following the expected bias voltage dependence.

Simulations using this model are also presented in Fig. 3 for the various distinct bias voltages. Various pulse cycles were mathematically executed up to attaining the convergence of the carrier densities in an equilibrium solution. The most important characteristics of the various transients including the nonexponential decays and the nonlinear effect are fairly reproduced using a reasonable set of time constants as presented in Table I. The nonlinear dependence introduced in the model has a strong effect on the low-energy emission, but it also has some reflection in the higher energy emission resulting in a clear delay of its transients even when the rate constants related to this transition are kept constant. The parameter $n_a(0)$ represents the initial number of electrons created at the accumulation layer by the laser pulse. We have used an increasing value of $n_a(0)$ with bias since the resulting increase in the electrical field in the structure should improve the probability that an electron created close to the surface drifts and accumulates adjacent to the AlAs barrier increasing the effective number of initial electrons created by a laser pulse at the accumulation layer. Most of the parameters were kept mainly constant at the low bias range where the transients present unusual characteristics with a major exception for $\tau_{\Gamma\text{-}X}$, which was chosen to be a minimum around 0.23 V, in agreement with the photocurrent peak attributed to the transfer of electrons from the $\Gamma$ GaAs accumulation layer to the $X$ AlAs layer. The tunneling time constant $\tau_{\Gamma\text{-}\Gamma}$ was kept constant for voltages smaller than 0.30 V;

TABLE I. Set of parameters used for the simulations of the PL transients presented in Fig. 3.

| | 0.21 | 0.22 | 0.23 | 0.26 | 0.34 | 0.68 | 1.54 |
|---|---|---|---|---|---|---|---|
| $n_a(0)$ | 0.5 | 5 | 20 | 40 | 50 | 50 | 50 |
| $n_a^*$ | 0.1 | 0.1 | 0.1 | 0.1 | 0.1 | 0.1 | 0.1 |
| $\Delta n_a$ | 1 | 1 | 1 | 1 | 1 | 1 | 1 |
| $\tau_{\Gamma\text{-}\Gamma}$ | 10 | 10 | 10 | 10 | 1 | 0.5 | 0.3 |
| $\tau_{\Gamma\text{-}X}$ | 50 | 5 | 5 | 9 | 15 | 50 | 80 |
| $\tau_{X\text{-}\Gamma}$ | 30 | 30 | 30 | 30 | 30 | 30 | 30 |
| $\tau_{iR}$ | 5 | 5 | 5 | 5 | 20 | 40 | 40 |
| $\tau_{dR}$ | 0.8 | 0.8 | 0.8 | 0.8 | 0.8 | 0.8 | 0.8 |
| $\tau_{\text{out}}$ | 0.1 | 0.1 | 0.1 | 0.1 | 0.1 | 0.1 | 0.1 |

but we have used decreasing values of $\tau_{\Gamma\text{-}\Gamma}$ for larger biases, since at this voltage the photocurrent signal associated to the Γ-Γ resonant tunneling of electrons to the first QW subband starts to emerge.

Alternative models with slightly distinct rate equations have also been tested, but most of them were not able to reproduce our experimental results, and the presented model is the simplest one that was able to simulate all results. Partial results were obtained using a similar model with the only difference that the concentration dependence of the indirect recombination rate $\tau_{iR}$ was supposed to be a function of the carrier density at the *X* AlAs subband instead of the carrier density at the accumulation layer. Physically, this assumption is very plausible, but the resulting system of differential equations is too critical and very often the concentrations diverged for a given set of parameters.

We can try to portray a simple picture for this complex system of differential equations. At low bias, the probability of direct Γ-Γ tunneling is still relatively small, and the alignment between the energy level at the accumulation layer and the *X* subband makes the Γ-*X* transfer a competitive path for electrons. In order to obtain the unusual evolution of the PL transients at this bias range, the *X*-Γ indirect-transition rate should present some nonlinear dependence on the density of carriers accumulated at the structure. Under those conditions, the relatively long-time constants associated to the indirect transitions as compared to the laser repetition generate an increasing number of carriers at the accumulation layer. Eventually, the system attains a point where a laser pulse drives the carrier density above a critical density, which instantaneously closes the indirect recombination path. The accumulated electrons are then slowly emptied through the Γ-Γ path, which is not very efficient at those voltages, and the indirect recombination rate slowly recovers its original value resulting in a slow increase in the indirect transition.

In summary, we have analyzed the dynamics of photocreated electrons in a *p*-*i*-*p* RTD. We observed clear evidences, both by transport and optical measurements, of an effective Γ-*X*-Γ tunneling of electrons through the double-barrier structure. Our measurements revealed that this alternative transport mechanism significantly affects the dynamics of the photocreated electrons along the structure. The photoluminescence transients from the QW are strongly delayed for bias voltages around the Γ-*X*-Γ transfer resonance bias resulting in a remarkable nonlinear effect where the emission intensity decreases at the arrival of a laser pulse. The transients were well reproduced by a simple model considering the rate equations of the Γ and *X* confined levels, where we introduced an upper limit for the density of electrons at the *X* AlAs level above which the formation of indirect excitons is strongly inhibited. Our results give additional insights on the Γ-*X*-Γ transfer mechanism and on its effect on RTDs structures based on AlAs layers.

We kindly acknowledge Peter A. Schulz for his valuable discussions. Financial support from Brazilian agencies FAPESP and CNPq and from the UK Engineering and Physical Sciences Research Council is gratefully acknowledged.

*Present address: Departamento de Física, Universidade Federal de Ouro Preto, 35400-000, Minas Gerais, Brazil.

[1] H. Mizuta and T. Tanoue, *The Physics and Applications of Resonant Tunneling Diodes* (Cambridge University Press, Cambridge, England, 1995).

[2] T. Koga, J. Nitta, H. Takayanagi, and S. Datta, Phys. Rev. Lett. **88**, 126601 (2002).

[3] A. Slobodskyy, C. Gould, T. Slobodskyy, C. R. Becker, G. Schmidt, and L. W. Molenkamp, Phys. Rev. Lett. **90**, 246601 (2003).

[4] M. M. Glazov, P. S. Alekseev, M. A. Odnoblyudov, V. M. Chistyakov, S. A. Tarasenko, and I. N. Yassievich, Phys. Rev. B **71**, 155313 (2005).

[5] H. B. de Carvalho, Y. Galvão Gobato, M. J. S. P. Brasil, V. Lopez-Richard, G. E. Marques, I. Camps, M. Henini, L. Eaves, and G. Hill, Phys. Rev. B **73**, 155317 (2006).

[6] H. B. de Carvalho, M. J. S. P. Brasil, Y. Galvão Gobato, G. E. Marques, H. V. A. Galeti, M. Henini, and G. Hill, Appl. Phys. Lett. **90**, 062120 (2007).

[7] E. E. Vdovin, Y. N. Khanin, L. Eaves, M. Henini, and G. Hill,

Phys. Rev. B **71**, 195320 (2005).
[8] E. E. Mendez, W. I. Wang, E. Calleja, and C. E. T. Gonçalves da Silva, Appl. Phys. Lett. **50**, 1263 (1987).
[9] A. R. Bonnefoi, T. C. McGill, R. D. Burnham, and G. B. Anderson, Appl. Phys. Lett. **50**, 44 (1987).
[10] J. J. Finley, R. J. Teissier, M. S. Skolnick, J. W. Cockburn, G. A. Roberts, R. Grey, G. Hill, M. A. Patê, and R. Planel, Phys. Rev. B **58**, 10619 (1998).
[11] H. Mimura, M. Hosoda, N. Ohtani, and K. Yokoo, Appl. Surf. Sci. **142**, 624 (1999).
[12] M. S. Skolnick, D. G. Hayes, P. E. Simmonds, A. W. Higgs, G. W. Smith, H. J. Hutchinson, C. R. Whitehouse, L. Eaves, M. Henini, O. H. Hughes, M. L. Leadbeater, and D. P. Halliday, Phys. Rev. B **41**, 10754 (1990).
[13] M. Tsuchiya, T. Matsusue, and H. Sakaki, Phys. Rev. Lett. **59**, 2356 (1987).
[14] C. Van Hoof, G. Borghs, and E. Goovaerts, Phys. Rev. B **46**, 6982 (1992).
[15] D. J. Lovering, G. J. Denton, A. Gregory, R. T. Phillips, M. S. Skolnick, A. W. Higgs, P. E. Simmonds, G. W. Smith, and C. R. Whitehouse, J. Phys.: Condens. Matter **5**, 2825 (1993).
[16] H. Käß, W. Schuddinck, E. Goovaerts, C. Van Hoof, and G. Borghs, Microelectron. Eng. **43**, 355 (1998).
[17] I. Romandic, A. Bouwen, E. Goovaerts, C. Van Hoof, and G. Borghs, Semicond. Sci. Technol. **15**, 665 (2000).
[18] R. K. Hayden, L. Eaves, M. Henini, D. K. Maude, and J. C. Portal, Phys. Rev. B **49**, 10745 (1994).